

Supplement data for:

Satellite observations reveal thirteen years of reservoir filling strategies, operating rules, and hydrological alterations in the Upper Mekong River Basin

Dung Trung Vu¹, Thanh Duc Dang^{1,2}, Stefano Galelli¹, and Faisal Hossain³

¹Pillar of Engineering Systems and Design, Singapore University of Technology and Design, Singapore

²Department of Civil and Environmental Engineering, University of South Florida, Tampa, FL, USA

³Department of Civil and Environmental Engineering, University of Washington, Seattle, WA, USA

Correspondence: Stefano Galelli (stefano_galelli@sutd.edu.sg)

Contents of this file

Tables S1 to S6

Figures S1 to S7

References

Table S1. Design specifications of the hydropower dams on the mainstream of the Lancang River. Retrieved from Do et al. (2020).

Name	Year of Commission	Dam Height (m)	Max WL (m a.s.l.)	Dead WL (m a.s.l.)	Max WSA (km ²)	Dead Storage (MCM)	Full Storage (MCM)	Hydropower Capacity (MW)
Jinghong	2009	108	602	595	510	810	1119	1750
Nuozhadu	2014	262	812	756	320	10414	21749	5850
Dachaoshan	2003	115	899	887	826	465	740	1350
Manwan	1992	132	994	982	415	630	887	1670
Xiaowan	2010	292	1236	1162	194	4750	14645	4200
Gongguoqiao	2012	105	1319	1311	343	196	316	900
Miaowei	2016	140	1408	1373	171	359	660	1400
Dahuaqiao	2018	106	1477	1466	148	252	293	920
Huangdeng	2017	203	1619	1604	199	1031	1418	1900
Tuoba	2023	158	1735	1725	177	735	1039	1400
Lidi	2019	74	1818	1813	4	57	71	420
Wunonglong	2018	138	1906	1894	163	236	272	990

WL Water level

WSA Water surface area

Table S2. Specifications of Landsat, MODIS and Sentinel images.

Satellite	Landsat (NASA and USGS)				MODIS (NASA)	Sentinel (ESA)		
	1-3	4-5	7	8		1	2	3
First Launch	1972	1982	1999	2013	1999	2014	2015	2016
Instrument	MSS	MSS, TM	ETM+	OLI, TIRS	MODIS	SAR	MSI	OLCI
Best Resolution	60 m	30 m	30 m	30 m	250 m	5 m	10 m	300 m
Frequency (Day)	16	16	16	16	1	12	10	27
Cloud Cover	Yes	Yes	Yes	Yes	Yes	No	Yes	Yes

MODIS Moderate Resolution Imaging Spectroradiometer

USGS United States Geological Survey

ESA European Space Agency

MSS Multi Spectral Scanner

TM Thematic Mapper

ETM+ Enhanced Thematic Mapper Plus

OLI Operational Land Imager

TIRS Thermal Infrared Sensor

SAR Synthetic Aperture Radar

MSI Multi-Spectral Instrument

OLCI Ocean and Land Colour Instrument

Table S3. Specifications of satellite altimeters.

Satellite	Type	Organization	Operation Time	Repeat Period (day)
Topex/Poseidon	Radar	NASA and CNES	1992-2002	10
Jason 1	Radar	NASA and CNES	2002-2008	10
Jason 2	Radar	NASA and CNES	2008-2016	10
Jason 3	Radar	NASA and CNES	2016-current	10
ERS 1	Radar	ESA	1992-1996	35
ERS 2	Radar	ESA	1996-2003	35
Envisat	Radar	ESA	2002-2010	35
SARAL	Radar	ISRO and CNES	2013-2016	35
Sentinel 3A	Radar	ESA	2016-current	27
Sentinel 3B	Radar	ESA	2018-current	27
ICESat 1	Laser	NASA	2003-2009	91
ICESat 2	Laser	NASA	2018-current	91

CNES National Centre for Space Studies

ESA European Space Agency

ISRO Indian Space Research Organization

ERS European Remote Sensing

SARAL Satellite with ARgos and ALtika

ICESat Ice, Cloud, and land Elevation Satellite

Table S4. Spectral indices for water surface extraction.

Index	Formula	Recommended Threshold Values
NDVI	(Red-Green)/(Red+Green)	0 (Zhai et al., 2015) and 0.1 (Gao et al., 2012)
NDWI	(Green-NIR)/(Green+NIR)	0 (Zhai et al., 2015), (Bonnema and Hossain, 2017)
MNDWI	(Green-MIR)/(Green+MIR)	0 and 0.1 (Duan and Bastiaanssen, 2013)

NDVI Normalized Difference Vegetation Index

NDWI Normalized Difference Water Index

MNDWI Modified Normalized Difference Water Index

NIR Near Infrared

MIR Middle Infrared

Table S5. Performance of the water surface area estimation algorithm for the reservoirs on the Lancang River.

Dry season (Dec-May)			
Reservoir	Number of	Percentage of Usable Images	
		Available Images	Before Improvement
Jinghong	175	24%	89%
Nuozhadu	187	27%	89%
Dachaoshan	187	26%	89%
Manwan	187	25%	85%
Xiaowan	187	27%	88%
Gongguoqiao	173	34%	75%
Miaowei	173	36%	84%
Dahuaqiao	173	36%	82%
Huangdeng	164	34%	85%
Wunonglong	164	34%	73%
Total	1770	30%	84%

Wet season (Jun-Nov)			
Reservoir	Number of	Percentage of Usable Images	
		Available Images	Before Improvement
Jinghong	122	20%	80%
Nuozhadu	127	13%	69%
Dachaoshan	130	16%	76%
Manwan	131	18%	77%
Xiaowan	130	16%	88%
Gongguoqiao	118	23%	69%
Miaowei	118	27%	90%
Dahuaqiao	118	28%	81%
Huangdeng	120	27%	78%
Wunonglong	120	20%	81%
Total	1234	21%	79%

Total			
Reservoir	Number of	Percentage of Usable Images	
		Available Images	Before Improvement
Jinghong	297	22%	85%
Nuozhadu	314	21%	81%
Dachaoshan	317	22%	84%
Manwan	318	22%	82%
Xiaowan	317	23%	88%
Gongguoqiao	291	29%	72%
Miaowei	291	32%	87%
Dahuaqiao	291	33%	81%
Huangdeng	284	31%	82%
Wunonglong	284	28%	76%
Total	3004	26%	82%

Table S6. The statistical indices of the annual peak discharge and lowest discharge discharge at Chiang Saen station for two periods before and after the two biggest dams (Nuozhadu and Xiaowan) began operations.

	Peak Discharge				Lowest Discharge			
	Mean	Q1	Median	Q3	Mean	Q1	Median	Q3
1990 - 2008	11157	9235	10700	12350	638	551	599	759
2013 - 2020	6476	5213	6834	7866	966	844	975	1077
Change	-45%	-45%	-43%	-42%	57%	69%	65%	42%

Figure S1. Performance of three spectral indices (NDVI, NDWI, and MNDWI) in extracting the water surface area of Xiaowan reservoir. Results are reported for three threshold values, 0, 0.05, and 0.1 and compared to the Maximum Water Extent dataset, developed by the European Commission's Joint Research Centre (Pekel et al., 2016). The meaning of the three indices is explained in Table S4.

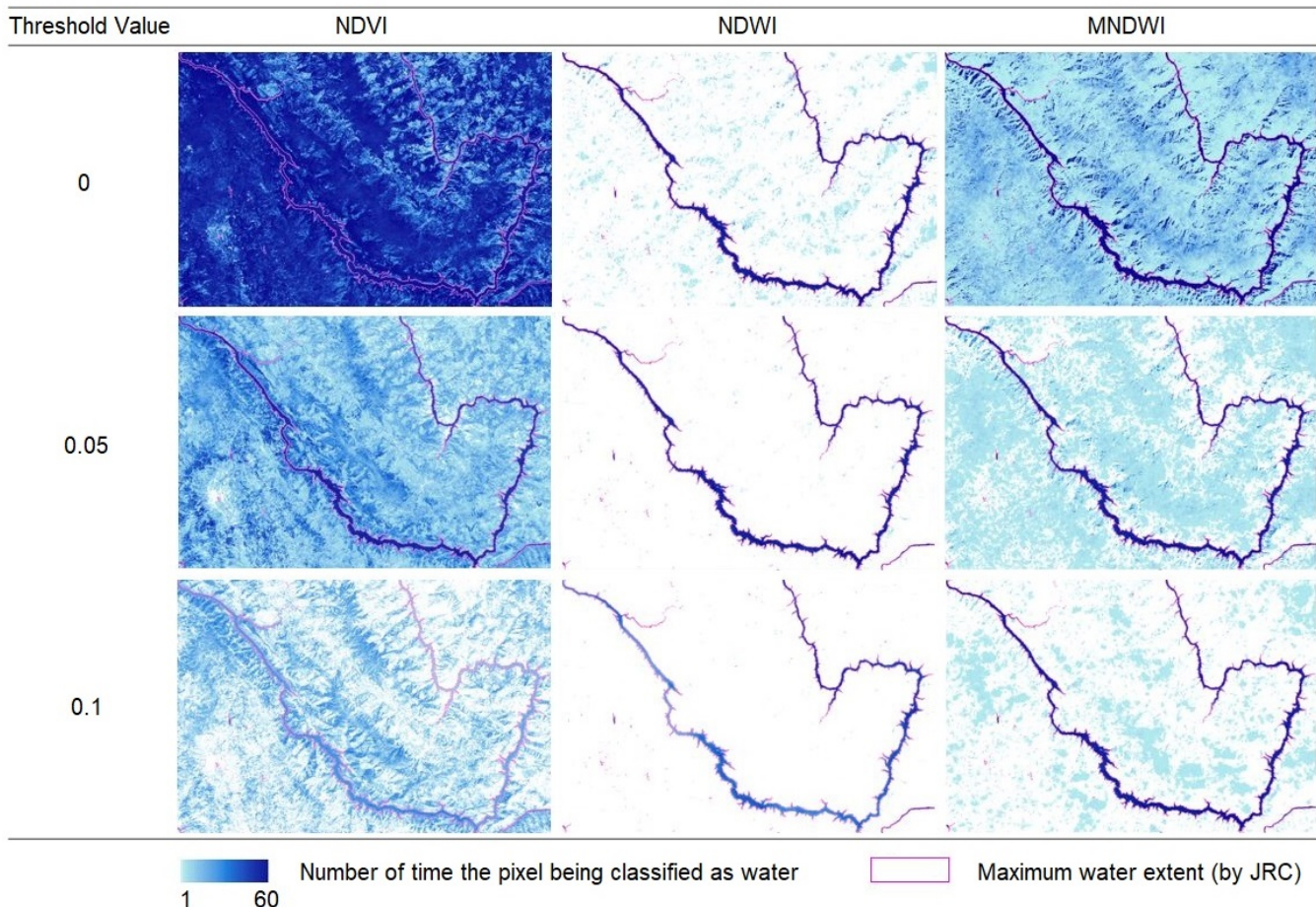


Figure S2. E-A, A-S and E-S curves of Jinghong, Dachaoshan, Manwan and Gongguoqiao reservoir.

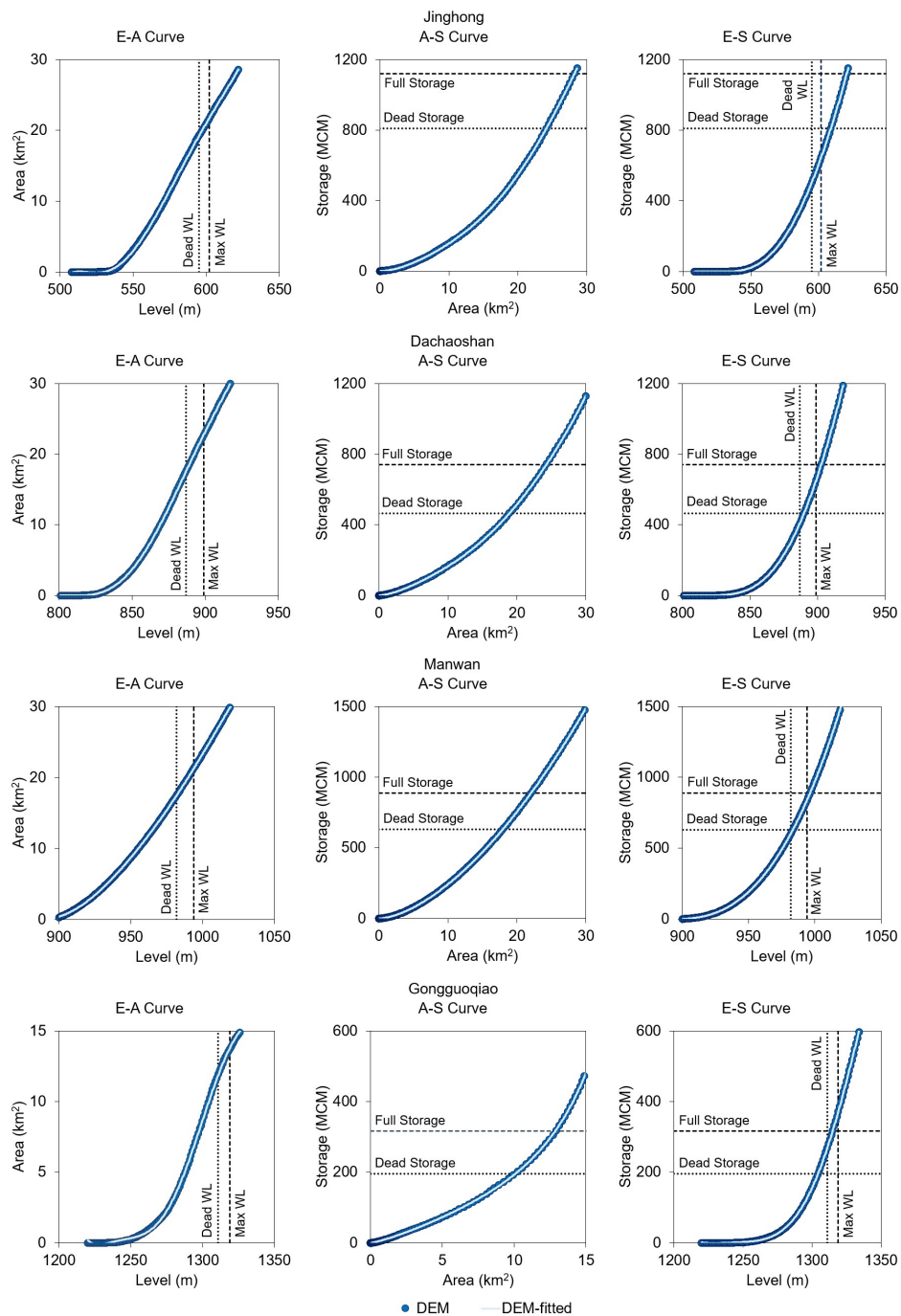


Figure S3. E-A, A-S and E-S curves of Miaowei, Dahuajiao, Huangdeng and Wunonglong reservoir.

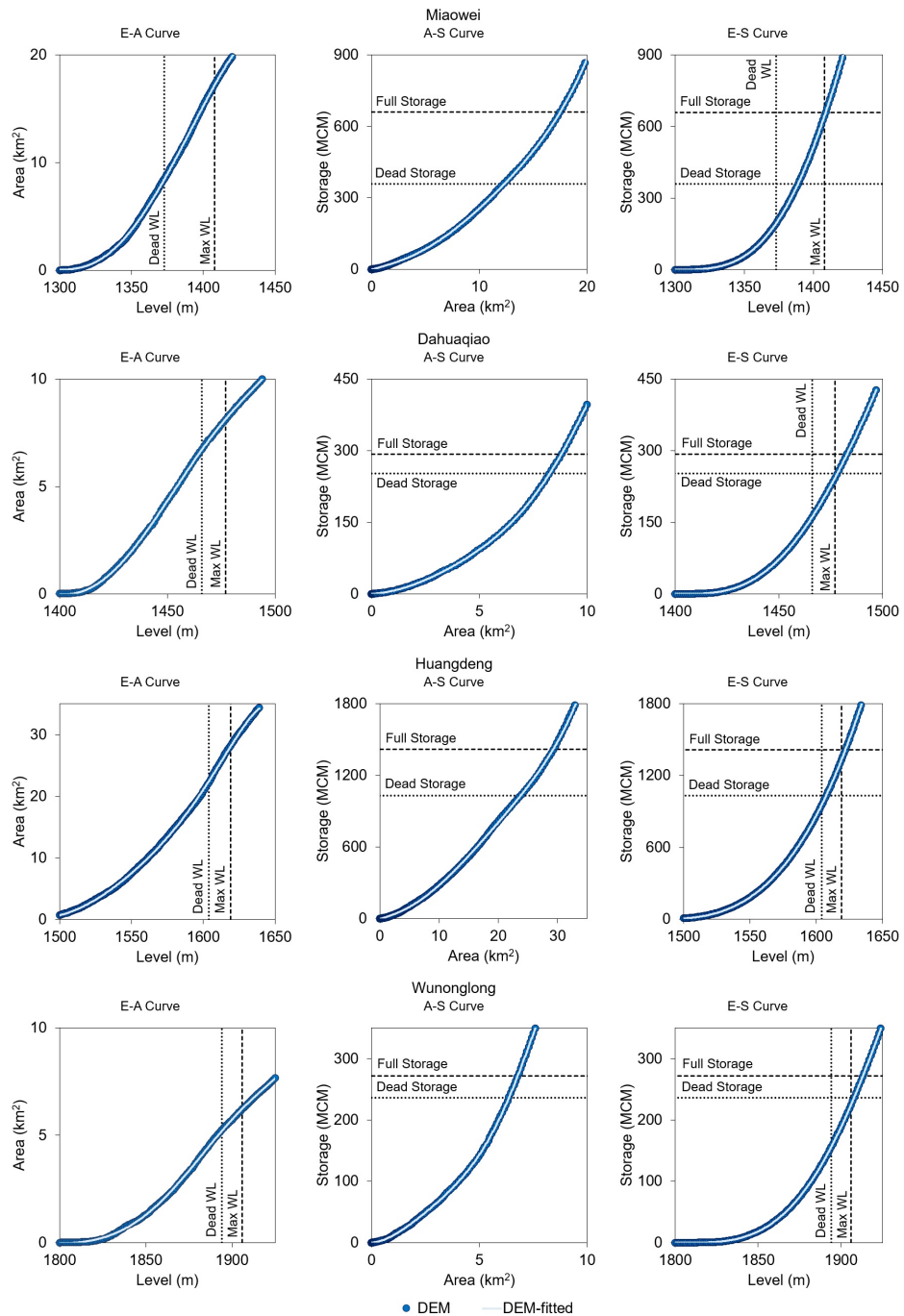


Figure S4. Storage variation of reservoir on the Lancang River.

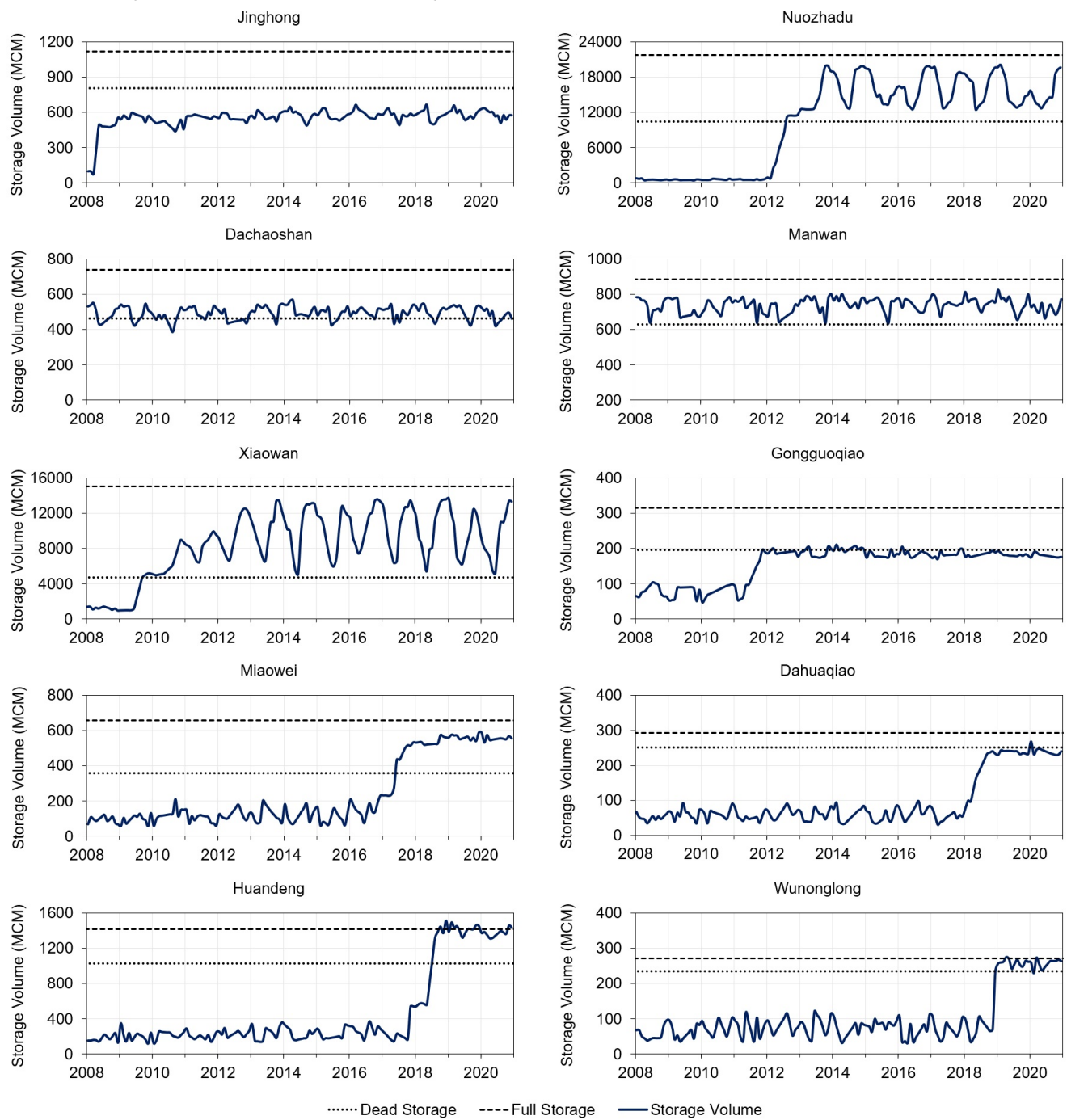


Figure S5. Comparison of storage derived from Landsat images and VIC-Res model for Nuozhadu (left) and Xiaowan (right) reservoirs.

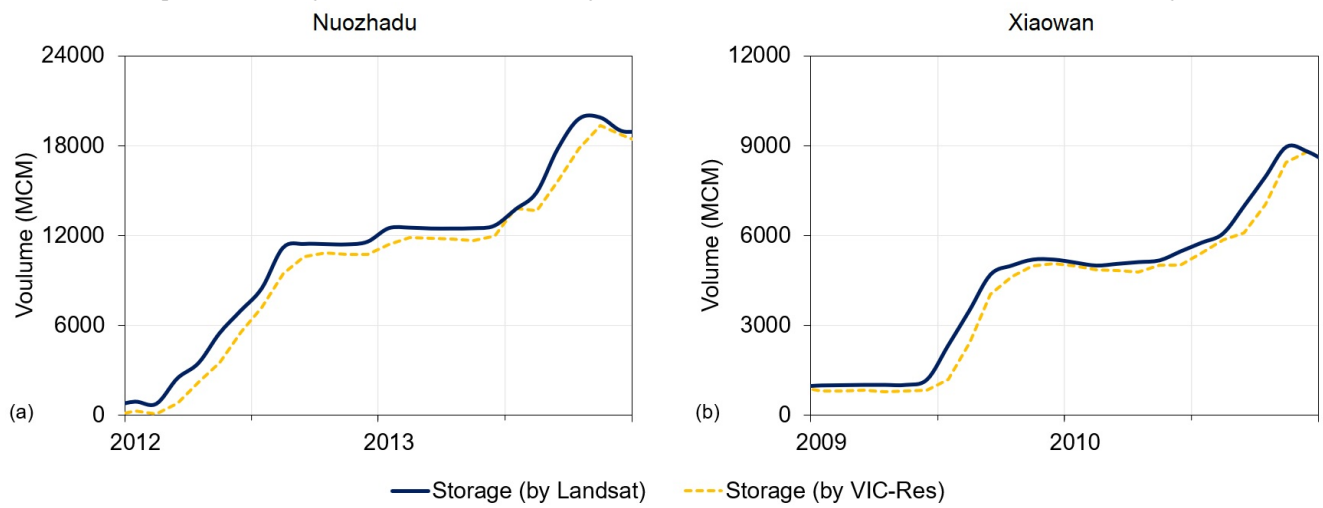


Figure S6. Operation curves of 8 reservoirs (Jinghong, Dachaoshan, Manwan, Gongguoqiao, Miaowei, Dahuaqiao, Huangdeng and Wunonglong).

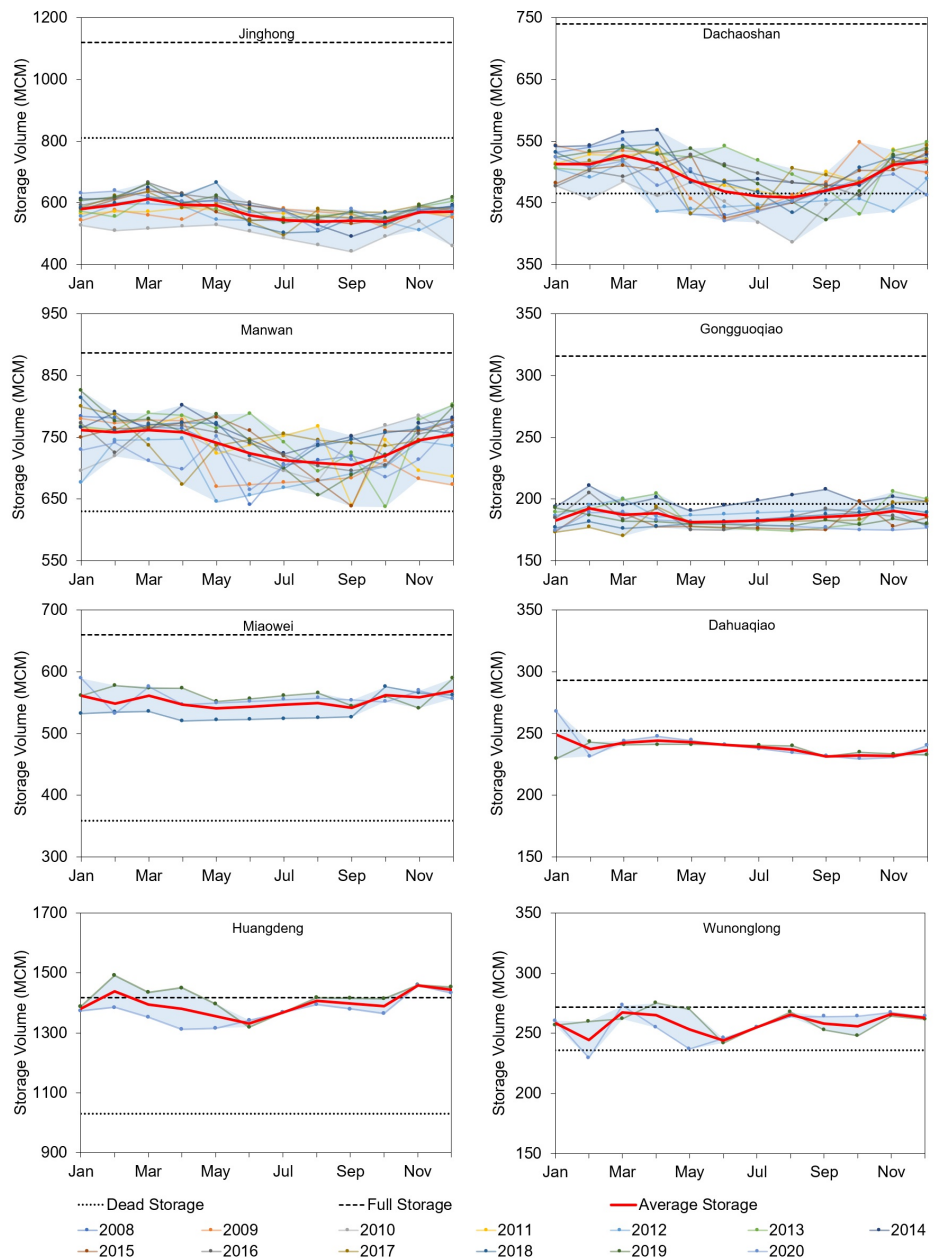
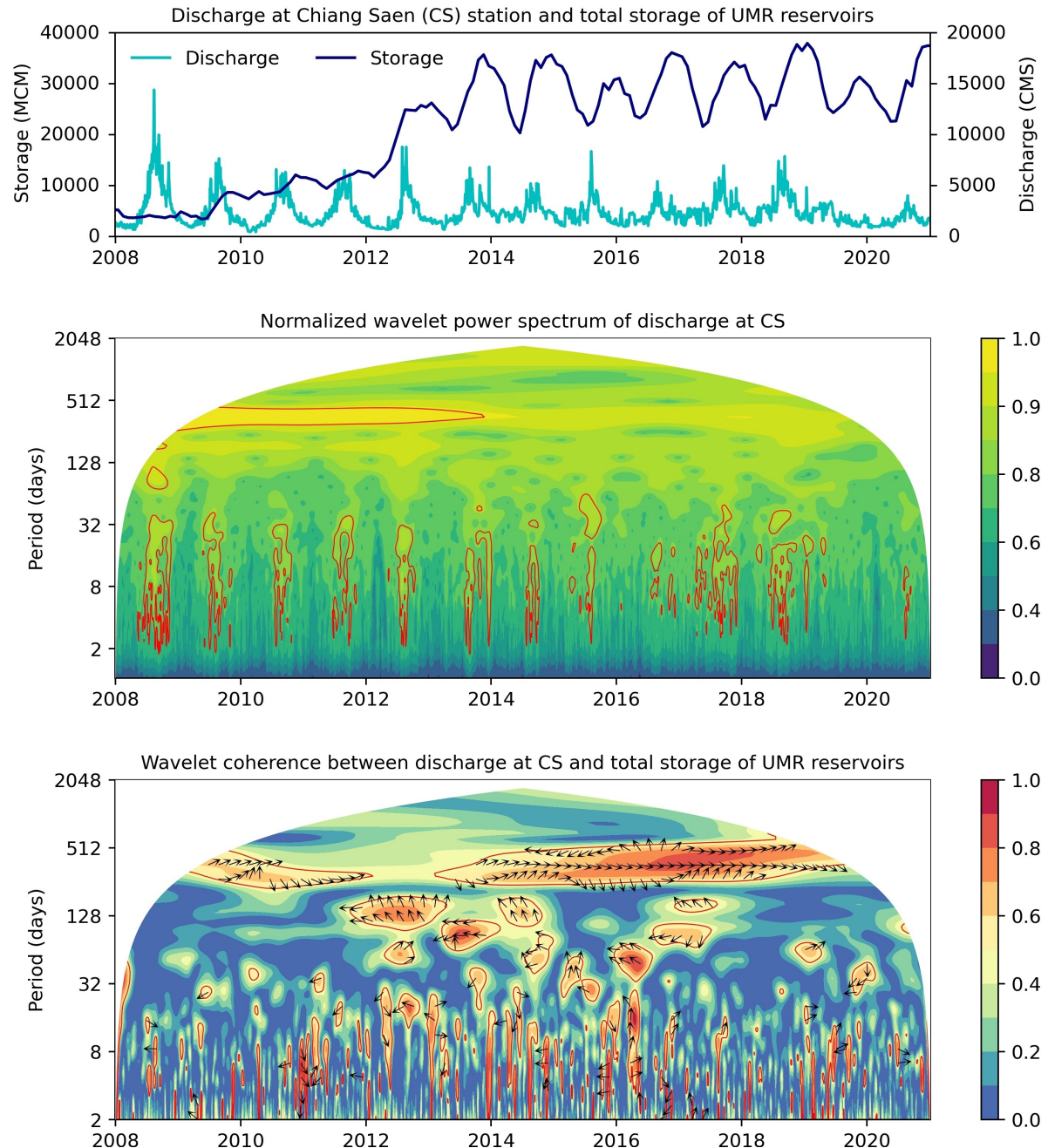


Figure S7. Upper panel: graphical illustration of total storage and discharge at Chiang Saen station. Middle panel: wavelet analysis of the discharge. Colors represent wavelet power, while confidence level contours identify statistically significant power. The flow regime changed in 2014, when Nuozhadu reservoir started its normal operations. Bottom panel: wavelet coherency and phase between discharge and reservoir storage. Contours identify statistically significant coherencies. The vectors indicate the phase difference between discharge and storage.



5 References

- Bonnema, M. and Hossain, F.: Inferring reservoir operating patterns across the Mekong Basin using only space observations, *Water Resources Research*, 53, 3791–3810, <https://doi.org/10.1002/2016wr019978>, 2017.
- Do, P., Tian, F., Zhu, T., Zohidov, B., Ni, G., Lu, H., and Liu, H.: Exploring synergies in the water-food-energy nexus by using an integrated hydro-economic optimization model for the Lancang-Mekong River Basin, *Science of The Total Environment*, 728, 137996, 10 <https://doi.org/10.1016/j.scitotenv.2020.137996>, 2020.
- Duan, Z. and Bastiaanssen, W. G. M.: Estimating water volume variations in lakes and reservoirs from four operational satellite altimetry databases and satellite imagery data, *Remote Sensing of Environment*, 134, 403–416, <https://doi.org/10.1016/j.rse.2013.03.010>, 2013.
- Gao, H., Birkett, C., and Lettenmaier, D. P.: Global monitoring of large reservoir storage from satellite remote sensing, *Water Resources Research*, 48, w09 504, <https://doi.org/10.1029/2012wr012063>, 2012.
- 15 Pekel, J.-F., Cottam, A., Gorelick, N., and Belward, A. S.: High-resolution mapping of global surface water and its long-term changes, *Nature*, 540, 418–422, <https://doi.org/10.1038/nature20584>, 2016.
- Zhai, K., Wu, X., Qin, Y., and Du, P.: Comparison of surface water extraction performances of different classic water indices using OLI and TM imageries in different situations, *Geospatial Information Science*, 18, 34–42, <https://doi.org/10.1080/10095020.2015.1017911>, 2015.